It is not immediately apparent that $f(n) = (k-n)/(1-n)$ represents a hyperbola; however, transforming this relation via the standard transformation-of-coordinates equations into a second, primed-coordinate system with origin at the center of the hyperbola and rotated as stated above will yield the transformed relation

$$\frac{n'^2}{2(k-1)} - \frac{f(n)'^2}{2(k-1)} = 1 \tag{7}$$

which, indeed, is the standard equation of an equilateral hyperbola with semitransverse and semiconjugate axes equal to $\sqrt{2(k-1)}$ and all other hyperbola characteristics now readily determinable.

However, and more importantly, from the thermodynamics point of view: Knowing that the polytropic specific heat equation represents a hyperbola, an overview of the complete range of c_n values now becomes readily available.

Application of Theory

Since certain actual expansion and compression processes of fluids may be described by a polytropic pressure-volume relationship as is the case in reciprocating compressors, for example, a numerical application of the presented theory to such a system is shown here in order to highlight the insight gained from the polytropic specific heat hyperbola.

Consider a reciprocating air compressor with inlet temperature and pressure of 294 K (530°R) and 1.01×10^5 N/m^2 (14.7 psia), respectively, having a compression ratio of 5, and a polytropic exponent $n = 1.35$.

For an ideal gas, substitution of the given conditions into the polytropic pressure-temperature relation

$$T_2/T_1 = (p_2/p_1)^{(n-1)/n} \tag{8}$$

yields a discharge temperature $T_2 = 447$ K (804°R) with $c_n = -0.0245$ kcal/kg·K (-0.005 Btu/lb·°R) directly readable from an enlarged Fig. 1, resulting in transferred heat $Q/m = -3.73$ kcal/kg (-6.71 Btu/lb). Allowing for a possible 10% uncertainty in n, the hyperbola indicates the more serious effects in the direction of decreasing n. Therefore, choosing $n = 1.22$ results in a discharge temperature $T_2 = 394$ K (709°R), a $c_n = -0.140$ kcal/kg·K (-0.029 Btu/lb.°R), and $Q/m = -13.9$ kcal/kg (-25.0 Btu/lb), representing a 273% change in transferred heat.

To explore the region of lesser sensitivity, consider a polytropic process with $n = 3$, initial temperature, and initial and final pressures as stated previously.

For this n, the polytropic relations yield $T_2 = 860$ K (1550°R), $c_n = 0.137$ kcal/kg·K (0.028 Btu/lb·°R), and a resultant unit mass heat transfer of $Q/m = 77.5$ kcal/kg (140 Btu/lb). Again, allowing for a 10% uncertainty in n, the hyperbola predicts a relatively small change in the transferred heat in the direction of increasing n. Indeed, $n = 3.3$ yields $T_2 = 904$ K (1630°R), $c_n = 0.142$ kcal/kg·K (0.029 Btu/lb·°R), and a unit mass heat transfer of $Q/m = 86.3$ kcal/kg (155 Btu/lb) which, by comparison with $n = 3$ values, represents a change of 11%.

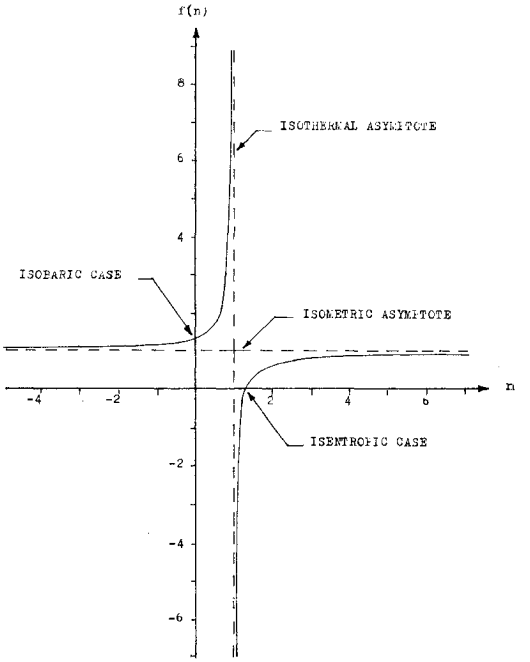

Fig. 1 Nondimensionalized polytropic specific heat hyperbola, $k = 1.4$.

Discussion and Conclusions

Figure 1 shows the nondimensionalized polytropic specific heat as a function of the polytropic exponent for $k = 1.4$, with the locations of the special-case processes identifed on the polytropic specific heat hyperbola.

Figure 1 also shows that the mathematical expression for the polytropic specific heat represents a translated and rotated equilateral hyperbola and, therefore, on the basis of just a few strategically determined data points it is possible to map out the entire range of the polytropic specific heat values, to discern by inspection the effects of small variations in n, and to determine if and where mean values are admissible.

The numerical examples presented show, as predicted by the polytropic specific heat hyperbola, that in the region of rapidly varying c_n, small changes in n, as they may occur in actual processes, produce significant changes in transferred heat, while in the region of lesser sensitivity the same variation in n produces correspondingly small changes in transferred heat.

While the ease with which the desired information may be obtained is obvious, perhaps the most significant insight offered by this graph is the realization of the effects of small fluctuations in n on c_n. When n is near 1 on either side, even minor deviations from its given value will produce substantial changes in the value of c_n, and in view of the fact that many actual fluid processes are governed by a polytropic pressure-volume relationship, to be able to identify critical regions in advance should be of decided advantage.

J80-136

Solar Flux Incident on an Orbiting Surface after Reflection from a Planet

70031
90005

Michael F. Modest*
Rensselaer Polytechnic Institute, Troy, N.Y.

Introduction

FOR spacecraft orbiting Earth or other planets, the incoming fluxes due to direct insolation, planetary (infrared) irradiation, and solar radiation reflected from the

Received April 24, 1979; revision received Oct. 23, 1979.

Index categories: Radiation and Radiative Heat Transfer; Spacecraft Temperature Control.

*Associate Professor of Mechanical Engineering, Dept. of Mechanical Engineering, Aeronautical Engineering and Mechanics.

planet (solar albedo) must be determined. While the calculation of direct insolation is trivial, determination of the other two components is more involved. If the planet is gray, diffuse, and spherical, planetary irradiation may be determined by calculating the radiation view factor between an infinitesimal area and a sphere, as was done by Cunningham.[1] To calculate the solar albedo flux it has been commonly assumed that the irradiated planet can be approximated by a large gray diffuse disk, often resulting in rather substantial errors. The present Note deals with the derivation of the algorithms describing the solar radiation impinging on an infinitesimal surface after reflection from a gray and diffuse planet. To avoid cumbersome numerical quadrature, a simple approximate formula is also presented below. As will be seen, the approximate relation displays surprising accuracy and should be sufficient for all practical applications.

Analysis

Let a body orbit around a planet of radius R, such as Earth, at an altitude Z. At the point on the surface of the orbiting body for which the incoming energy flux, i.e., solar energy reflected from the planet, is to be calculated a coordinate system is introduced consisting of two perpendicular surface tangents $\hat{t}_1$ and $\hat{t}_2$, and the outward surface normal $\hat{n}$, all of unit length. The relative position of the planet and the direction toward the sun may be fixed by unit vectors pointed toward the centers of planet and sun, respectively (cf. Fig. 1):

$$\hat{s}_p = \sin\beta_p\cos\theta_p\ \hat{t}_1 + \sin\beta_p\sin\theta_p\ \hat{t}_2 + \cos\beta_p\hat{n} \tag{1}$$

$$\hat{s}_s = \sin\beta_s\cos\theta_s\ \hat{t}_1 + \sin\beta_s\sin\theta_s\ \hat{t}_2 + \cos\beta_s\hat{n} \tag{2}$$

where β and θ are polar and azimuth angles in the $\hat{t}_1 - \hat{t}_2 - \hat{n}$ coordinate system, respectively. In order to determine from what directions β, θ the reflected radiation from the sunny half of the planet is incident upon the orbiting surface, another coordinate system is introduced at the center of the planet consisting of three perpendicular unit vectors $\hat{\tau}_1$, $\hat{\tau}_2$, and $\hat{s}_s$. Choosing

$$\hat{\tau}_1 = \hat{s}_s \times \hat{n}/\sin\beta_s \quad \text{and} \quad \hat{\tau}_2 = \hat{s}_s \times \hat{\tau}_1 \tag{3}$$

a unit vector from the center of the planet pointing to its surface can be formed as

$$\hat{r} = \sin\alpha\sin\psi\ \hat{\tau}_1 + \sin\alpha\cos\psi\ \hat{\tau}_2 + \cos\alpha\hat{s}_s \tag{4}$$

A unit vector from the orbiting surface to the surface of the planet follows then as

$$\hat{s}(\beta,\theta) = [(R+Z)\hat{s}_p + R\hat{r}(\alpha,\psi)]/S \tag{5}$$

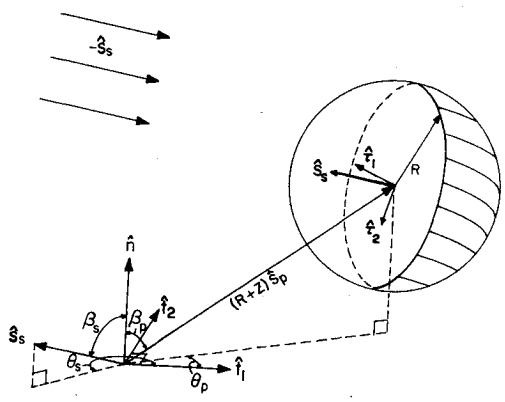

Fig. 1 Coordinate system for surface orbiting a planet.

where S is the distance from the orbiting body to the surface of the planet, and β and θ are the polar and azimuthal angles of $\hat{s}$, respectively. For sunlight reflected from the sunny half of the planet that falls on the top of the orbiting surface, the following conditions must be satisfied:

$$\alpha \le \pi/2; \quad \beta \le \pi/2; \quad (S/R) \le (S/R)_{\max} = \cot\gamma \tag{6}$$

The first condition assures that only radiation from the sunny half of the planet is taken into account. The second condition specifies that the radiation must fall on the top of the orbiting surface. Finally, the third condition states that radiation must come from that part of the planet that can be seen from the orbiting body (γ is the angle between $\hat{s}_p$ and a tangent to the planet surface). Thus, relations (5) and (6) specify the ranges of β and θ from which reflected solar energy is incident on the orbiting surface. The total incident flux may now be calculated from[2]

$$q = \int_0^\infty \int_\Omega i'_{r\lambda}(\hat{s})\,\hat{n}\cdot\hat{s}\,\mathrm{d}\omega(\hat{s})\,\mathrm{d}\lambda \tag{7}$$

where Ω is the total solid angle with which the sunny half of the planet is seen, and $i'_{r\lambda}$ is the spectral intensity of the reflected sunshine. Assuming a uniform, gray, and diffuse reflectivity ρ_p for the planet, Eq. (7) reduces to

$$\mathcal{F} \equiv \frac{q}{\rho_p q_s} = \frac{1}{\pi}\int_{\beta_{\min}}^{\beta_{\max}}\int_{\theta_{\min}(\beta)}^{\theta_{\max}(\beta)} \cos\alpha(\beta,\theta)\cos\beta\sin\beta\,\mathrm{d}\theta\,\mathrm{d}\beta \tag{8}$$

where q_s is the solar constant. Note that Eq. (8) is the view factor from an infinitesimal area element to a semisphere except for the $\cos\alpha$ in the integrand. This term is due to the fact that the amount of solar energy intercepted by the planetary surface varies with interception angle α. The $\cos\alpha$ may be expressed in terms of β and θ as

$$\cos\alpha = [\sin\beta\sin\beta_s\cos(\theta-\theta_s) + \cos\beta\cos\beta_s](S/R) - [\sin\beta_p\sin\beta_s\cos(\theta_p-\theta_s) + \cos\beta_p\cos\beta_s]/\sin\gamma \tag{9}$$

$$(S/R) = [\sin\beta\sin\beta_p\cos(\theta_p-\theta) + \cos\beta\cos\beta_p]/\sin\gamma - [(\sin\beta\sin\beta_p\cos(\theta_p-\theta) + \cos\beta\cos\beta_p)^2/\sin^2\gamma - \cot^2\gamma]^{1/2} \tag{10}$$

It does not appear possible to express the allowable range for the angles β and θ in explicit formulae. To minimize computational effort it is advantageous to initially calculate the range for $\bar{\beta}$, $\bar{\theta}$ from which the entire planet is seen [i.e., dropping the condition that $\alpha \le \pi/2$]. This determination is straightforward and results in

$$\bar{\beta}_{\min} = \begin{cases} 0\ , & 0 \le \beta_p \le \gamma \\ \beta_p - \gamma, & \gamma \le \beta_p \le (\pi/2) + \gamma \end{cases} \tag{11}$$

$$\bar{\beta}_{\max} = \begin{cases} \beta_p + \gamma\ , & 0 \le \beta_p \le (\pi/2) - \gamma \\ \pi/2\ , & (\pi/2) - \gamma \le \beta_p \le (\pi/2) + \gamma \end{cases} \tag{12}$$

$$\theta_p - \bar{\theta}_{\min} = \bar{\theta}_{\max} - \theta_p = \begin{cases} \pi\ , & \bar{\beta}_{\min} \le \beta \le \gamma - \beta_p \\ \cos^{-1}\left[\dfrac{\cos\gamma - \cos\beta_p\cos\beta}{\sin\beta_p\sin\beta}\right], & \gamma - \beta_p \le \beta \le \bar{\beta}_{\max} \end{cases} \tag{13}$$

It is now a relatively simple matter to modify the limiting values for β and θ by imposing the additional condition $\alpha \leq (\pi/2)$. While implicit relations for the limiting values for β and θ can be found from Eqs. (9) through (13), this turns out to be rather cumbersome. In view of the fact that Eq. (8) must be integrated numerically anyway, it is much more convenient to rewrite Eq. (8) as

$$\mathfrak{F} \equiv \frac{q}{\alpha_p q_s} = \frac{1}{\pi} \int_{\beta_{\min}}^{\bar{\beta}_{\min}} \int_{\theta_{\min}}^{\theta_{\max}} f\,[\alpha(\beta,\theta)] \cos\beta \sin\beta \, d\theta \, d\beta \tag{14}$$

$$f\,[\alpha(\beta,\theta)] = \begin{cases} \cos\alpha(\beta,\theta) & \cos\alpha \geq 0 \\ 0 & \cos\alpha \leq 0 \end{cases} \tag{15}$$

where the full-planet limits from Eqs. (11-13) are used. Equation (14) is now readily evaluated by numerical quadrature.

A more detailed account of the above analysis may be found in Ref. 3. For Monte Carlo calculations Eq. (14) may also be used to determine random numbers R_β and R_θ for the incident directions β, θ. This equation has been applied in Refs. 4 and 5 and is also described in detail in Ref. 3.

Results and Discussion

It is obvious from Eq. (14) that the solar reflection exchange factor $q/\rho_p q_s$ is a function of four parameters: β_p, β_s, $|\theta_p - \theta_s|$, and γ. Thus space limitations do not permit a complete tabulation in this publication. A few graphs are shown here that demonstrate the general trends and make it possible to evaluate the most important, i.e., largest, exchange factors. Figure 2 shows the case of the orbiting surface directly facing the planet ($\beta_p = 0$ deg) as a function of orbiting radius with sun polar angle β_s as parameter. If the sun is incident from well behind the orbiting surface, the surface sees essentially an evenly illuminated disk and the exchange factor decreases monotonically with orbiting radius. If the sun comes from the side or even above the orbiting surface, the exchange factor first increases with orbiting radius before it decreases. The results are compared with the assumption that the entire planet is evenly illuminated, i.e., $\cos\alpha = \cos\bar{\alpha} = \text{const}$, where $\bar{\alpha}$ is evaluated at the point on the planet which is closest to the orbiting surface, i.e.,

$$\cos\bar{\alpha} = -\hat{s}_p \cdot \hat{s}_s = \cos\beta_p \cos\beta_s - \sin\beta_p \sin\beta_s \cos(\theta_p - \theta_s) \tag{16}$$

With this assumption, Eq. (8) reduces to

$$\mathfrak{F} = (q/\rho_p q_s) \cong F_{dA-p} \cos\bar{\alpha} \tag{17}$$

where F_{dA-p} is the view factor between a small surface and a large sphere as reported by Cunningham[1]:

$$F_{dA-p} = \begin{cases} \sin^2\gamma \cos\beta_p & 0 \leq \beta_p \leq (\pi/2) - \gamma \\ [\sin^2\gamma \cos\beta_p \cos^{-1}(-\cot\gamma \cot\beta_p) & \\ \quad + \cos^{-1}(\cos\gamma/\sin\beta_p) - \cos\gamma\sqrt{\sin^2\gamma - \cos^2\beta_p}]/\pi & \\ & (\pi/2) - \gamma \leq \beta_p \leq (\pi/2) + \gamma \end{cases} \tag{18}$$

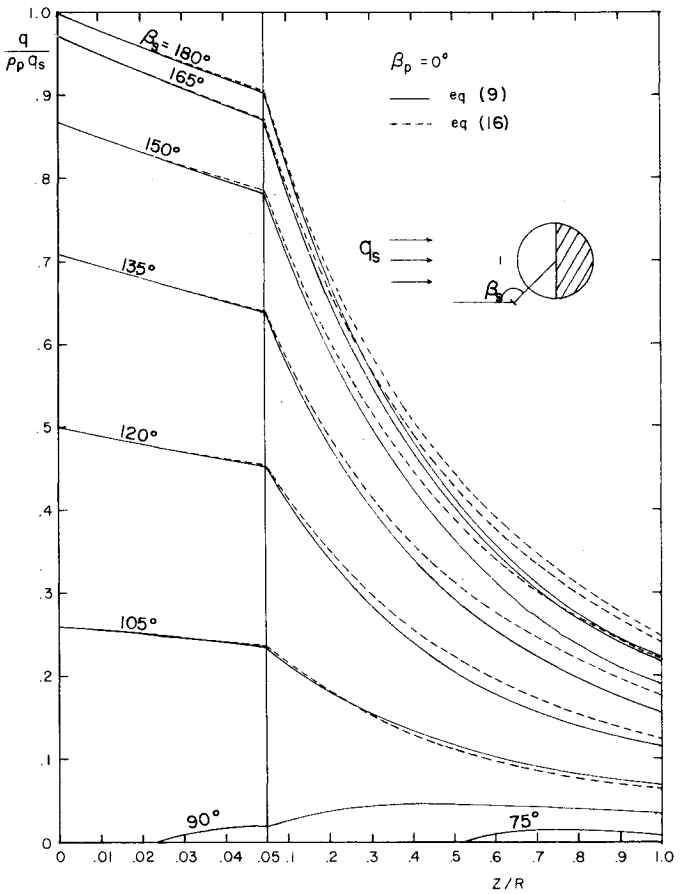

Fig. 2 Solar albedo flux on a surface directly facing planet.

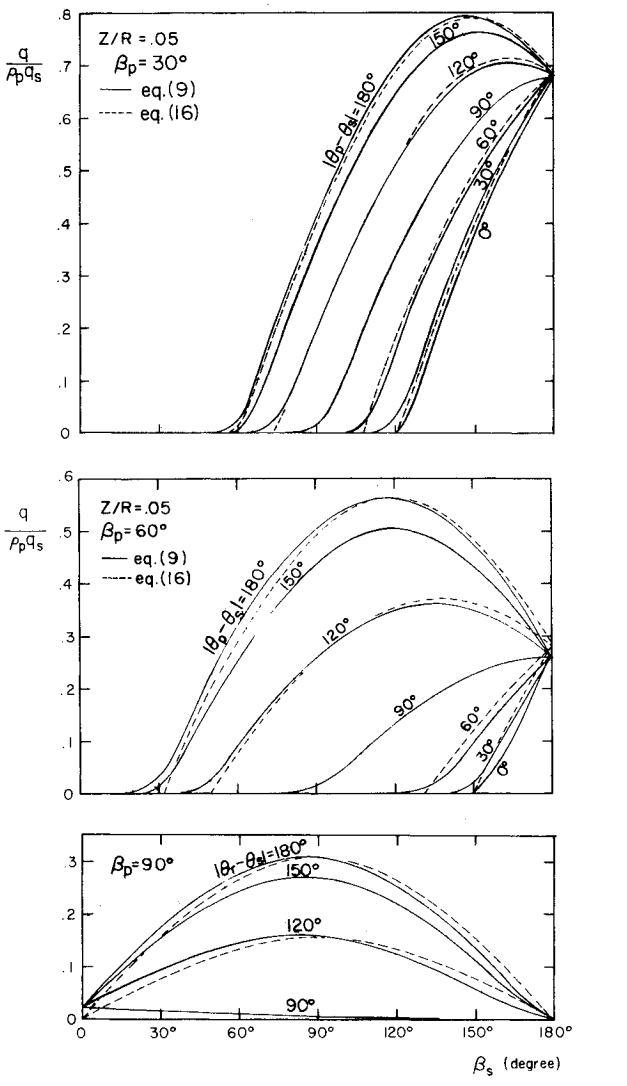

Fig. 3 Influence of solar position on albedo flux.

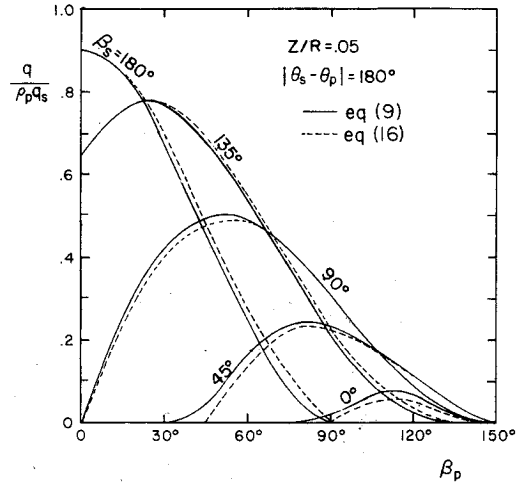

Fig. 4 Solar albedo flux as function of surface-planet tilt angle β_p.

It is seen that whenever $\mathfrak{F}$ is appreciable the approximate result yields excellent accuracy. The error is never larger than 0.05. Only when $\mathfrak{F}$ is very small does the relative error become large: for $\beta_s \leq 90$ deg Eq. (17) predicts $\mathfrak{F} \leq 0$, and $\mathfrak{F}$ should be set equal to zero.

In the following figures $Z = 0.05$ R was chosen as a typical orbit. Figure 3 shows the influence of solar position β_s and θ_s. It is seen that the reflected solar flux is a maximum near the direction where $\cos\tilde{\alpha}$ is a maximum, i.e., at

$$\tan\beta_s = \tan\beta_p \cos(\theta_p - \theta_s) \tag{19}$$

This is the reason why the approximation, Eq. (17), is so successful as is seen again in this figure. (For clarity the approximate solution is not shown for all cases.)

A final comparison is shown in Fig. 4 for sun and planet on opposing sides, $|\theta_p - \theta_s| = 180$ deg with sun polar angle β_s as parameter. The approximate maxima are again given by Eq. (19), i.e., $\beta_s + \beta_p = 180$ deg. As before, the approximation gives excellent results for all cases.

The simple approximate formula displays excellent accuracy for all significant situations, with an error which is always less than 5% of the maximum possible reflected flux. It is felt that this approximation is adequate for all practical applications as the common and concurrent assumption of a gray and diffuse planet results in errors of at least the same magnitude.

Acknowledgment

This research was made possible in part by NASA Grant NAS9-15109.

References

[1] Cunningham, F. G., "Power Input to a Small Flat Plate from a Diffusely Radiating Sphere, With Application to Earth Satellites," NASA TN D-710, 1961.

[2] Siegel, R. and Howell, J. R., *Thermal Radiation Heat Transfer*, McGraw-Hill, New York, 1972.

[3] Modest, M. F., "Computer Code MCDREF-User's Manual (Monte Carlo Determination of Radiative Exchange Factors)," Crew Systems Division, NASA-JSC, Contract No. NAS9-15109, Houston, Texas, 1979.

[4] Modest, M. F. and Poon, S. C., "Determination of Three-Dimensional Radiative Exchange Factors for the Space Shuttle by Monte Carlo," ASME Paper 77-HT-49, 1977.

[5] Modest, M. F., "Three-Dimensional Radiative Exchange Factors for Nongray, Nondiffuse Surfaces," *Numerical Heat Transfer*, Vol. 1, 1978, pp. 403-416.

J80-137

90005
90010

Emittance of a Finite Scattering Medium with Refractive Index Greater Than Unity

A.L. Crosbie*
University of Missouri-Rolla, Rolla, Mo.

Introduction

REFRACTIVE index and scattering can significantly influence the transfer or radiation in a semitransparent medium such as water, glass, plastics, or ceramics. In a recent article,[1] the author presented exact numerical results for the emittance of a semi-infinite scattering medium with a refractive index greater than unity. The objective of the present investigation is to extend the analysis to a finite medium.

Formulation

The physical situation consists of a finite planar layer. The isothermal layer emits, absorbs, and isotropically scatters thermal radiation. It is characterized by a single scattering albedo ω, an optical thickness τ_0, a refractive index n, and a temperature T. The interface at $\tau = 0$ is assumed to be smooth and its reflection and transmission characteristics are governed by Snell's law and the Fresnel relations. The bottom ($\tau = \tau_0$) is transparent. The intensity incident on the interface from inside the medium is given by[1]

$$I^-(0,\mu) = n^2 I_b(T)\epsilon_m(\mu) + 2\int_0^1 \rho(\mu') I^-(0,\mu')\rho_m(\mu,\mu')\mu' d\mu' \tag{1}$$

where μ is the cosine of the polar angle inside the medium, $I_b(T)$ is the Planck function, and $\rho(\mu)$ is the interface reflectance. Physically, $\epsilon_m(\mu)$ and $\rho_m(\mu,\mu_0)$ are the directional emittance and the bidirectional reflectance, respectively, of a finite medium with a refractive index of unity. These properties are simply related to Chandrasekhar's X and Y functions[2,3]:

$$\rho_m(\mu,\mu_0) = (\omega/4)\,[X(\mu;\tau_0)X(\mu_0;\tau_0) - Y(\mu;\tau_0)\,Y(\mu_0;\tau_0)\,]/(\mu+\mu_0) \tag{2}$$

$$\epsilon_m(\mu) = \left(1 - \frac{\omega}{2}\alpha_0 - \frac{\omega}{2}\beta_0\right)[X(\mu;\tau_0) - Y(\mu;\tau_0)] \tag{3}$$

where the moments are defined as

$$\alpha_0 = \int_0^1 X(\mu;\tau_0)\,d\mu \text{ and } \beta_0 = \int_0^1 Y(\mu;\tau_0)\,d\mu.$$

Since integral Eq. (1) is linear, $I^-(0,\mu)$ can be expressed in terms of a universal function $f(\mu)$, i.e., $I^-(0,\mu) = n^2 I_b(T)$

Received Aug. 21, 1979; revision received Oct. 29, 1979.

Index categories: Radiation and Radiative Heat Transfer; Thermal Surface Properties.

*Professor, Thermal Radiative Transfer Group, Dept. of Mechanical and Aerospace Engineering. Member AIAA.